

Negative thermal expansion in cubic ZrW_2O_8 : Role of phonons in the entire Brillouin zone from *ab initio* calculations

M. K. Gupta, R. Mittal, and S. L. Chaplot

Solid State Physics Division, Bhabha Atomic Research Centre, Trombay, Mumbai 400 085, India

(Received 10 April 2013; revised manuscript received 13 June 2013; published 15 July 2013)

We report the *ab initio* density functional theory calculation of phonons in the cubic phase of ZrW_2O_8 in the entire Brillouin zone and identify specific anharmonic phonons that are responsible for large negative thermal expansion (NTE) in terms of the translation, rotation, and distortion of WO_4 and ZrO_6 . We have used density functional calculations to interpret the experimental phonon spectra as a function of pressure and temperature as reported in literature. We discover that the phonons showing anharmonicity with temperature are not necessarily the same as those showing anharmonicity with pressure although both are of similar frequencies. Only the latter phonons are associated with NTE. Therefore, the cubic and/or quadratic anharmonicity of phonons is not relevant to NTE but just the volume dependence of frequencies. The calculations are able to reproduce the observed anomalous trends, namely, the softening of the low-frequency peak at about 4 meV in the phonon spectra with pressure and its hardening with temperature, whereas, both changes involve a compression of the lattice.

DOI: [10.1103/PhysRevB.88.014303](https://doi.org/10.1103/PhysRevB.88.014303)

PACS number(s): 63.20.dk, 65.40.-b

The discovery of large isotropic negative thermal expansion (NTE) in the cubic phase of ZrW_2O_8 two decades ago has led to great excitement in the field of material science. Since then, anomalous thermal expansion behavior has been found in a large number of open frame work compounds.¹⁻³ ZrW_2O_8 has $M\text{-O-}M'$ ($M, M' = \text{Zr, W}$) types of linkages and shows¹ a negative volume thermal expansion coefficient of $-29 \times 10^{-6} \text{ K}^{-1}$ at 300 K. Increasing flexibility in the structure has led to the discovery of compounds exhibiting⁴ colossal positive and negative thermal expansions. The compounds find applications in forming the composites with tailored thermal expansion coefficients useful for applications, such as in fiber-optic communication systems.

At ambient pressure, ZrW_2O_8 crystallizes¹ in a cubic structure ($P2_13$, $Z = 4$) that consists of ZrO_6 octahedral and WO_4 tetrahedral units. Diffraction, spectroscopic, as well as computer simulation techniques⁵⁻¹² have been used to understand the thermodynamic behavior of ZrW_2O_8 . All these papers show that the anharmonicity of low-energy phonon modes has a major contribution to the observed thermal expansion behavior. X-ray absorption fine-structure measurements¹² led to a suggestion that NTE in ZrW_2O_8 could be due to the translational motion of WO_4 tetrahedra along the $\langle 111 \rangle$ axis along with the correlated motion of three nearest ZrO_6 octahedra. The reverse Monte Carlo analysis of the neutron-total-scattering data suggested¹⁰ that WO_4 as well as ZrO_6 polyhedra rotate and translate as rigid units. Earlier, a rigid unit mode model¹⁰ was also used to understand the NTE behavior of ZrW_2O_8 . Hancock *et al.*¹¹ proposed other modes involving translation and rotation of polyhedra. It seems all the phonon modes identified from various techniques could contribute to NTE.

Earlier neutron-scattering data⁹ as well as theoretical⁸ estimates of the anharmonicity of the phonons in ZrW_2O_8 using the interatomic potential model indicated that modes of energy below 8 meV are responsible for observed NTE. However, estimates based on Raman spectroscopy showed⁷ that several modes up to 50 meV contribute to NTE. The large disagreement in the energy range as well as the nature of the

low-energy modes in previous papers indicated the need for an understanding of the NTE behavior in ZrW_2O_8 using *ab initio* calculations. Recently, *ab initio* calculations of zone-center phonon modes have been published.⁶ However, the authors concluded⁶ that one should fully explore the nature of the phonons in the entire Brillouin zone for understanding the mechanism of NTE. Here, we report such a comprehensive calculation and identify specific zone-boundary modes that are highly anharmonic. The calculations are able to reproduce the observed NTE as well as anomalous trends of the phonon spectra with increases in temperature and pressure.

Important soft modes were identified in cubic ReO_3 (Ref. 13) and ScF_3 (Ref. 14) at M and R points, respectively, in the Brillouin zone. These modes simultaneously show both a large negative Grüneisen parameter as well as a large quadratic anharmonicity, the former leading to NTE, and the latter leading to the temperature dependence. In the case of ZrW_2O_8 , we find that the modes that show the large negative Grüneisen parameter and contribute to NTE are not necessarily the same as those showing cubic and/or quadratic anharmonicity and significant temperature dependence. This finding means that the modes found to be anharmonic in temperature-dependent measurements are not necessarily relevant to NTE.

The first-principles calculations of the lattice dynamics have been performed using the Vienna *ab initio* simulation package¹⁵⁻¹⁸ and the PHONON5.2 software.¹⁹ The details are given in the Supplemental Material.²⁰ The calculations reproduce the equilibrium crystal structural parameters, elastic constants, and mean-squared amplitude of various atoms quite satisfactorily as given in Tables SI and SII of the Supplemental Material.²⁰

The calculated phonon spectrum is found to be in excellent agreement with the experimental phonon spectrum⁵ as shown in Fig. 1. The calculated energies of all the zone-center modes are also shown in Fig. 1. The calculated partial density of states of various atoms shows (Fig. S1 of Ref. 20) that vibrations due to Zr atoms span only up to 50 meV, whereas, vibrations due to W and O span the entire energy range. The W-O stretching modes lie in the energy range from 85 to 130 meV.

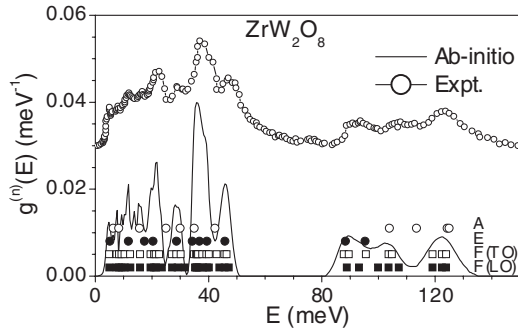


FIG. 1. The calculated (0 K) and experimental (300 K) (Ref. 5) neutron-weighted phonon spectra in ZrW_2O_8 . The phonon spectra are normalized to unity. For better visibility, the experimental phonon spectra⁵ are shifted along the y axis by 0.03 meV^{-1} . The calculated zone-center optic modes A , E , $F(\text{TO})$, and $F(\text{LO})$ are also shown. TO and LO correspond to transverse optic and longitudinal optic modes respectively.

The calculated phonon dispersion relation along the high-symmetry directions is shown in Fig. S2.²⁰ The low-energy range of phonon dispersion up to 50 meV contains large number of nondispersive phonon branches, which give rise to several peaks in the density of states. To emphasize the anharmonic nature of low-energy phonons, we have also shown the phonon dispersion up to 10 meV (Fig. 2) at 0 and 1 kbar. We find that several phonon branches soften with increasing pressure. The lowest optic mode is calculated at 40 cm^{-1} ($\sim 5 \text{ meV}$), which is in excellent agreement with the experimental value of 40 cm^{-1} from Raman spectroscopic studies⁷ as well as infrared measurements.⁶ The optic modes along with several phonon branches give rise to the first peak in the calculated phonon density of states at 4.5 meV, which is observed at 3.8 meV in neutron-scattering experiments.⁵ The low-energy peak also leads to a sharp increase in the specific heat at low temperatures [Fig. S3 (Ref. 20)]. The good agreement between our calculated and experimental specific heat^{21,22} supports the correctness of the low-energy phonon density of states provided by the *ab initio* calculations.

The calculation of thermal expansion is carried out using the quasiharmonic approximation. Each phonon mode of energy E_i contributes to the volume thermal expansion coefficient²³ that is given by the relation $\alpha_V = \frac{1}{B} \sum_i \Gamma_{iT} C_{Vi}(T)$, where V is the unit-cell volume, B is the bulk modulus,

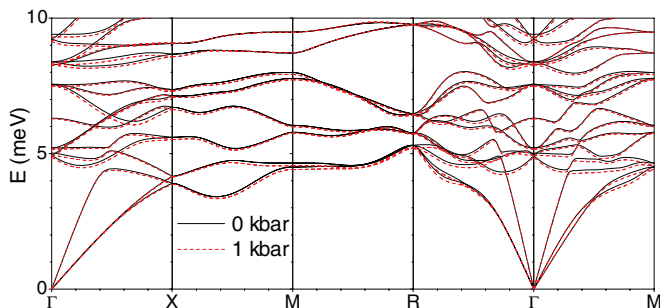


FIG. 2. (Color online) Calculated low-energy part of the pressure-dependent dispersion relation for ZrW_2O_8 . $\Gamma = (0,0,0)$; $X = (1/2,0,0)$; $M = (1/2,1/2,0)$; and $R = (1/2,1/2,1/2)$.

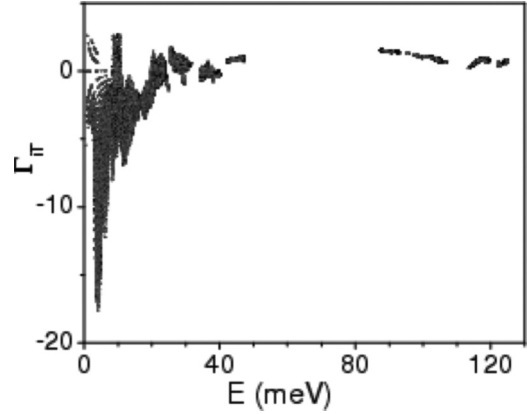


FIG. 3. The calculated Grüneisen parameters as a function of phonon energy.

Γ_{iT} ($= -\partial \ln E_i / \partial \ln V$) are the mode Grüneisen parameters, and C_{Vi} is the specific-heat contribution of the phonons of energy E_i . The index i runs over the various phonon branches and all the wave vectors in the Brillouin zone. The Grüneisen parameters Γ_{iT} (Fig. 3) are numerically calculated from the pressure dependence of phonon modes around ambient pressure.

The calculated α_V at 300 K from the *ab initio* calculation is $-22.5 \times 10^{-6} \text{ K}^{-1}$, whereas, the experimental value¹ is about $-29 \times 10^{-6} \text{ K}^{-1}$. The calculated relative volume thermal expansion is shown in Fig. 4(a). The discontinuity in the experimental data at about 400 K is associated with an order-disorder phase transition. We find that there is a slight deviation between the experimental data¹ and the calculations at low temperatures due to the underestimation of the contribution from low-energy phonon modes. A similar underestimation of the anharmonicity of low-energy phonon modes is also found in cases of $\text{Zn}(\text{CN})_2$ (Ref. 24) as well as $\text{Ag}_3\text{M}(\text{CN})_6$ ($M = \text{Co}, \text{Fe}$).²⁵ The properties of the low-energy phonon modes are very sensitive to the volume of the crystal. Density functional theory calculations overestimate or underestimate crystal volume depending on the exchange-correlation functional.

The contribution of the phonon density of states at energy E to the thermal expansion has been determined [Fig. 4(b)] as a

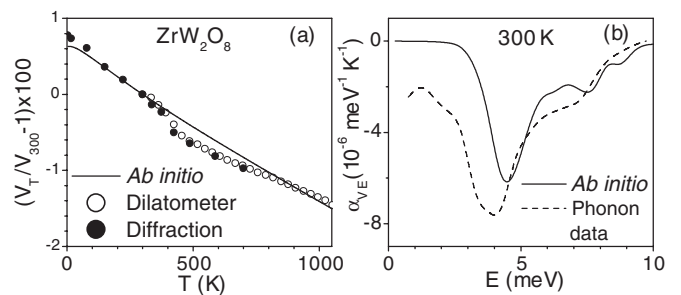


FIG. 4. (a) The calculated and experimental¹ relative volume thermal expansion for ZrW_2O_8 , $(V_T/V_{300} - 1) \times 100\%$, V_T and V_{300} being the cell volumes at temperatures T and 300 K, respectively. There is a small drop in volume at about 400 K associated with an order-disorder phase transition. (b) The contribution of the phonons of energy E to the volume thermal expansion as a function of E at 300 K from the *ab initio* calculation as well as the phonon data.⁹

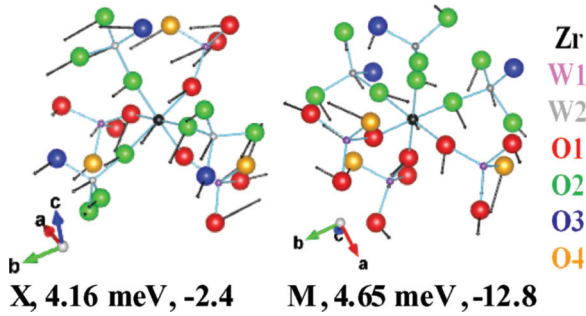


FIG. 5. (Color online) Polarization vectors of selected phonon modes in ZrW_2O_8 . The numbers after the wave vectors (X and M) give the phonon energies and Grüneisen parameters, respectively. The lengths of the arrows are related to the displacements of the atoms. The atoms are labeled as indicated in Ref. 1.

function of phonon energy at 300 K. We find that the maximum contribution to α_V is found to be from phonon modes of energy 4.5 ± 1 meV, which is consistent with the previous analysis of high-pressure inelastic-neutron-scattering measurements⁹ as well as diffraction data.⁵

The eigenvectors of a few of the low-energy modes (Table I) that contribute most to NTE have also been plotted (Figs. 5 and S4). The nature of these phonons can be best understood by the animations which are available in the Supplemental Material.²⁰ The lowest Γ -point mode of 4.93 meV ($\Gamma_{IT} = -7.0$) involves the out-of-phase translation of two chains consisting of WO_4 and ZrO_6 , whereas, the Γ -point mode of 5.21 meV ($\Gamma_{IT} = -5.7$) shows the out-of-phase rotation of WO_4 and the translation of ZrO_6 in two different chains. These modes also involve significant distortion of WO_4 tetrahedra formed around W1 and W2.

Hancock *et al.*¹¹ proposed two types of modes for understanding the mechanism of NTE. In one of the modes, both ZrO_6 as well as WO_4 in a chain rotate and translate along the $\langle 111 \rangle$ axis. As discussed above, for the two lowest optic modes, we have not found simultaneous rotational motion of both ZrO_6 as well as WO_4 . However, we find that, for the X -point modes of 3.90 meV ($\Gamma_{IT} = -5.7$) and 4.16 meV ($\Gamma_{IT} = -2.4$), the motion of the polyhedral units is similar to that proposed by Hancock *et al.*¹¹ The modes show in-phase translation and rotation of WO_4 and ZrO_6 in a single chain. The motion of tetrahedral and octahedral units in two different chains is also in phase. Although the two modes seem to be of a similar nature, the relative amplitudes of Zr, W, and O atoms are found to be different.

The second mode proposed by Hancock *et al.*¹¹ indicates that the ZrO_6 octahedron rotates opposite to the WO_4 tetrahedra. We find that the R -point (0.5 0.5 0.5) mode of 5.29 meV with a Γ_{IT} value of -11.7 shows a similar behavior. The two WO_4 's around W1 and W2 in a chain rotate in phase, whereas, ZrO_6 rotates out of phase. In general, we find that, in most of the modes, the amplitude of the free oxygens O3 and O4 are larger as compared to that of the shared oxygens O1 and O2. This means that the rotation of WO_4 and ZrO_6 is accompanied by a distortion of these polyhedra.

The M -point modes of 4.51- and 4.65-meV energy have a negative Grüneisen parameter Γ_{IT} value of about -12.7 and -12.8 , respectively. The mode at 4.51 meV involves in-phase

translation and bending of the WO_4 and ZrO_6 networks. The mode is very similar to that previously described by Cao *et al.*¹² where a correlated motion between WO_4 and its nearest ZrO_6 is shown to lead NTE. However, for the 4.65-meV mode, we find out-of-phase translation of WO_4 and ZrO_6 in two chains.

The temperature dependence of the phonon density of states of ZrW_2O_8 shows⁵ hardening of the peak at 3.8–4.05 meV on an increase in temperature from 50 to 300 K. On the other hand, the same peak is found to soften with pressure,⁹ although both increases in pressure and temperature involve compression of the lattice. Temperature and pressure variations in the phonon energy are known to occur due to anharmonicity of the interatomic potential. The change in phonon energies is due to two effects. The so-called “implicit” anharmonicity refers to the volume dependence of the phonon spectra that can be calculated in the quasiharmonic approximation. The second is the “explicit” anharmonicity, which refers to the changes in phonon frequencies due to the large thermal amplitude of the atoms. The change in phonon energies with temperature is due to both the implicit as well as the explicit anharmonicities, whereas, the pressure effect only involves the implicit part. We would also call the implicit and explicit parts volume and amplitude effects, respectively.

In a complex crystal, it is quite difficult to rigorously estimate the anharmonic effects. However, one can make certain simplifying assumptions and can arrive at qualitative trends in the shifts in selected phonons as a function of temperature. The potential wells of a few of the phonon modes at high-symmetry points in the cubic Brillouin zone have been calculated and have been used to estimate the temperature dependence of the phonon frequencies. The detailed procedure for the calculation of the explicit part of the temperature dependence of the phonon modes can be found in the Supplemental Material²⁰ as well as in Refs. 26–28.

The potential wells (Figs. 6 and S5) of the seven modes of energy around 4.5 meV along the high-symmetry points, namely, Γ , X , M , and R in the cubic Brillouin zone, have been calculated. The energy of the modes may increase or decrease with increases in temperature, depending on the nature of the anharmonicity. The potential wells for the Γ -point mode of energy at 4.93 and 5.21 meV (Table SIII) have cubic as well as quadratic anharmonicities, whereas, all the remaining five modes only have quadratic anharmonicity. The potential well for the M -point mode of 4.65 meV with the Grüneisen parameter Γ_{IT} value of about -12.7 has also been plotted at

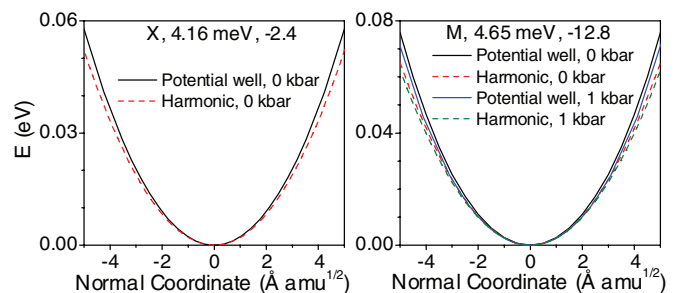


FIG. 6. (Color online) Calculated potential wells of selected phonon modes in ZrW_2O_8 . The numbers after the wave vectors (X and M) give the phonon energies and Grüneisen parameters, respectively.

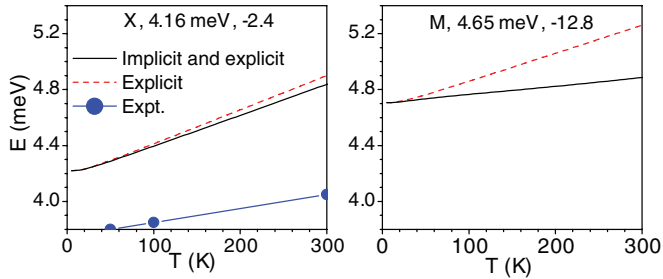


FIG. 7. (Color online) Calculated temperature dependence of selected phonon modes in ZrW_2O_8 . The numbers after the wave vectors (X and M) give the phonon energies and Grüneisen parameters, respectively. For comparison, the experimental temperature dependence of the phonon peak at 3.8 meV in the density of states⁵ is also shown, which involves an average over the entire Brillouin zone.

1 kbar. As expected, the width of the well is slightly increased due to the softening of the phonon mode on compression.

The anharmonicity parameters (Table SIII) as obtained from the fitting of Eq. (S1) to the potential well are used for calculating the temperature dependence of the phonon modes. We find (Figs. 7 and S6) that the zone-boundary mode of energy 4.16 meV (0 K) at the X point shows maximum hardening and shifts to 4.78 meV on increases in temperature to 300 K. The low-energy Γ -point modes do not respond to temperature and remain nearly invariant with temperature. The R -point mode of energy, 5.29 meV, shows the normal behavior of a decrease in phonon energy with an increase in temperature. The calculated energy shift for low-energy modes on an increase in temperature from 0 to 300 K is given in Table I. *Ab initio* calculations are able to qualitatively explain the experimentally observed⁵ temperature dependence of the low-energy phonon spectra of ZrW_2O_8 (Fig. 7).

We would like to draw attention to the fact that the modes at the M and R points show large implicit anharmonicity. These modes are important for understanding the NTE behavior. However, as far as temperature dependence is concerned, the X -point mode, having a low negative Grüneisen parameter Γ_{iT} value of -2.4 , shows maximum temperature dependence.

TABLE I. The calculated change in energy of selected phonon modes on increases in temperature from 0 to 300 K. E_i and Γ_{iT} are the phonon energy at 0 K and the Grüneisen parameter. ΔE_V and ΔE_A are the changes in the phonon energy due to a change in volume (implicit anharmonicity) and due to an increase in the thermal amplitudes of the atoms (explicit anharmonicity), respectively, and ΔE_T is the total change in the phonon energy. All the energy values are in meV units.

Wave vector	E_i	Γ_{iT}	ΔE_V	ΔE_A	ΔE_T
Γ	4.93	-7.0	-0.22	0.15	-0.07
Γ	5.21	-5.7	-0.19	0.16	-0.03
X	3.90	-5.7	-0.14	0.22	0.08
X	4.16	-2.4	-0.06	0.68	0.62
M	4.51	-12.7	-0.36	0.42	0.06
M	4.65	-12.8	-0.37	0.55	0.18
R	5.29	-11.7	-0.39	-0.38	-0.77

Recently, in the case of NTE compounds ScF_3 (Ref. 14) and ReO_3 (Ref. 13), respectively, R -point and M -point modes are found to show high pressure as well as temperature dependence. The authors also found large quadratic anharmonicity for the same modes. We would like to say that quadratic anharmonicity is useful for explaining the large temperature dependence of the R -point and M -point modes and is not relevant to NTE.

To summarize, the *ab initio* density functional calculations of the phonons modes of ZrW_2O_8 have been reported in the entire Brillouin zone. Certain phonon modes are found to be highly anharmonic in nature. The calculations agree quite well with the reported NTE behavior of ZrW_2O_8 . We have also been able to explain the observed anomalous pressure as well as the temperature variation in the energies of the phonon modes. The increase in the frequency with temperature essentially results from the cubic and/or quadratic anharmonic part of the phonon potential, which is able to explain the temperature dependence of the low-energy modes as reported in the literature.

¹T. A. Mary, J. S. O. Evans, T. Vogt, and A. W. Sleight, *Science* **272**, 90 (1996).

²B. K. Greve, K. L. Martin, P. L. Lee, P. J. Chupas, K. W. Chapman, and A. P. Wilkinson, *J. Am. Chem. Soc.* **132**, 15496 (2010).

³C. Lind, A. P. Wilkinson, Z. Hu, S. Short, and J. D. Jorgensen, *Chem. Mater.* **10**, 2335 (1998).

⁴A. L. Goodwin, D. A. Keen, M. G. Tucker, M. T. Dove, L. Peters, and J. S. O. Evans, *J. Am. Chem. Soc.* **130**, 9660 (2008).

⁵G. Ernst, C. Broholm, G. R. Kowach, and A. P. Ramirez, *Nature (London)* **396**, 147 (1998).

⁶V. Gava, A. L. Martinotto, and C. A. Perottoni, *Phys. Rev. Lett.* **109**, 195503 (2012).

⁷T. R. Ravindran, A. K. Arora, and T. A. Mary, *Phys. Rev. Lett.* **84**, 3879 (2000).

⁸R. Mittal and S. L. Chaplot, *Phys. Rev. B* **60**, 7234 (1999).

⁹R. Mittal, S. L. Chaplot, H. Schober, and T. A. Mary, *Phys. Rev. Lett.* **86**, 4692 (2001).

¹⁰M. G. Tucker, A. L. Goodwin, M. T. Dove, D. A. Keen, S. A. Wells, and J. S. O. Evans, *Phys. Rev. Lett.* **95**, 255501 (2005); A. K. A. Pryde, K. D. Hammonds, M. T. Dove, V. Heine, J. D. Gale, and M. C. Warren, *J. Phys.: Condens. Matter* **8**, 10973 (1996).

¹¹J. N. Hancock, C. Turpen, Z. Schlesinger, G. R. Kowach, and A. P. Ramirez, *Phys. Rev. Lett.* **93**, 225501 (2004).

¹²D. Cao, F. Bridges, G. R. Kowach, and A. P. Ramirez, *Phys. Rev. Lett.* **89**, 215902 (2002).

¹³T. Chatterji, P. G. Freeman, M. Jimenez-Ruiz, R. Mittal, and S. L. Chaplot, *Phys. Rev. B* **79**, 184302 (2009).

¹⁴C. W. Li, X. Tang, J. A. Muñoz, J. B. Keith, S. J. Tracy, D. L. Abernathy, and B. Fultz, *Phys. Rev. Lett.* **107**, 195504 (2011).

¹⁵G. Kresse and J. Furthmüller, *Comput. Mater. Sci.* **6**, 15 (1996).

- ¹⁶G. Kresse and D. Joubert, *Phys. Rev. B* **59**, 1758 (1999).
- ¹⁷J. P. Perdew, K. Burke, and M. Ernzerhof, *Phys. Rev. Lett.* **77**, 3865 (1996).
- ¹⁸J. P. Perdew, K. Burke, and M. Ernzerhof, *Phys. Rev. Lett.* **78**, 1396 (1997).
- ¹⁹K. Parlinski, PHONON software (2003).
- ²⁰See Supplemental Material at <http://link.aps.org/supplemental/10.1103/PhysRevB.88.014303> for details about the *ab initio* calculations, the calculation of the explicit part of the temperature dependence of phonon frequencies, the other results from the *ab initio* calculations, and the animation of modes.
- ²¹A. P. Ramirez and G. R. Kowach, *Phys. Rev. Lett.* **80**, 4903 (1998).
- ²²Y. Yamamura, N. Nakajima, T. Tsuji, M. Koyano, Y. Iwasa, S. Katayama, K. Saito, and M. Sorai, *Phys. Rev. B* **66**, 014301 (2002).
- ²³G. Venkataraman, L. Feldkamp, and V. C. Sahni, *Dynamics of Perfect Crystals* (MIT Press, Cambridge, MA, 1975).
- ²⁴R. Mittal, M. Zbiri, H. Schober, E. Marelli, S. J. Hibble, A. M. Chippindale, and S. L. Chaplot, *Phys. Rev. B* **83**, 024301 (2011).
- ²⁵R. Mittal, M. Zbiri, H. Schober, S. N. Achary, A. K. Tyagi, and S. L. Chaplot, *J. Phys.: Condens. Matter* **24**, 505404 (2012).
- ²⁶N. Choudhury, S. L. Chaplot, and K. R. Rao, *Phys. Rev. B* **33**, 8607 (1986).
- ²⁷B. Kuchta and T. Luty, *Chem. Phys. Lett.* **92**, 462 (1982).
- ²⁸B. Kuchta and T. Luty, *J. Chem. Phys.* **78**, 1447 (1983).